An Analytic Study on the Enhancement of Heat Transfer with Nanofluid

Bhuvaneswari SUBRAMANIAN [1], **Elatharasan GOVINDARAJ** [2] *,

Mukesh Kumar PERIYASAMY CHOKKAYEE AMMAL [3]

[1] *University College of Engineering, Pattukkottai, Rajamadam-614701, Tamilnadu, India*

[2] *Department of Mechanical Engineering, University College of Engineering, Pattukkottai, Rajamadam-614701, Tamilnadu, India*

[3] *Department of Mechanical Engineering, University College of Engineering, Dindigul, ReddiyarChattram, Dindigul-624622, Tamilnadu, India*

The article studies the problem of boundary layer fluid flow for two dimensional steady and incompressible hybrid nanofluids over the nonlinear stretching surface. The problem is analysed for the distribution of velocity, temperature, and concentration profile influenced by the parameters taken for study. The pertinent parameters analysed in the boundary value problem are magnetic, non-linear stretching parameter, Prandtl number, radiation, Brownian, thermophoresis. The governing sets of PDE's are converted to a set of ODES using the similarity transformations. The numerical results are obtained by RK algorithm techniques. The study portrays the results for skin friction and Nusselt number for varying the parametric values. The interpretation of results is done graphically and in tabular format. The detailed parametric study is explored for the enhancement of heat transfer, the influence of the parameters on velocity, temperature, and volume fraction of the nanofluid, skin friction coefficient, and Nusselt number. The wide applications of the problem taken for the study where the control of complex parametric influence in heat transfer is applied in the field of energy recovery, biomedical, and industrial systems in the present global scenario.

Keywords: heat transfer, hybrid nanofluid, nonlinear stretching sheet, boundary value problem.

1. INTRODUCTION

The process of transmission of heat in the field of thermal that deals with the conversion, exchange, generation of thermal energy and heat with actual structures. The three broad classifications of heat transfer are thermal radiation, conduction, and convection. Heat convection deals with fluid flow, which transports heat with materials in motion. Mass transfer considered the movement of mass from one stream, phase, or component to another, is a key concept in heat transmission. A nanofluid has a varied range of practical applications in the fields of engineering, technology, and science, with its ability to enhance thermal conductivity. These applications are making a significant impact, from improving the efficiency of heat exchangers to enhancing the performance of electronic devices. Substances of solid particles are present in the base fluid, further enhancing thermal conductivity and thermal transmission. The natural transfer of heat mass through convection in a Newtonian fluid with initial cooling of the cryogenic surface, in the presence of thermal diffusion and Soret effects in the two-dimensional form [1], is just one example of the practical applications of nanofluids. The two-dimensional Newtonian steady state fluid of the boundary layer was studied for the mixed laminar convection with the vertical and continuously stretching sheet [2, 3]. Using the shifted Legendre collocation method, a numerical technique for solving differential equations, boundary layer fluid flows stretched out on a sheet

containing Casson fluid that has different thicknesses, conductivity, and radiative heat. Heat transfer enhancement with dusty fluid for the semi-infinite isothermal plate together with the supported boundary initial conditions along with heat radiation and slip conditions over a curved surface [4 – 7].

Numerical investigation of Sisko nanofluid analysed for the heat transfer over a nonlinear surface influenced by the consequence of thermophoresis and Brownian motion [8, 9]. The analysis of the saturated porous medium's buoyancy-induced flows for the non-permeable surface with stagnation flow of the fluid across the shrinking sheet with the development of suction provides not only theoretical insights into the reduction in skin friction over an extension in the sheet and increment in skin friction when there is an increase in suction factor but also has practical implications. It sheds light on the influence of the magneto hydrodynamic flow of boundary layer problems with the chemical reaction past nonlinear stretching sheet together with the thermal radiation [10, 11]. Experimental work on the convectively heated surface of non-linearity with the MHD three-dimensional fluid flows for the boundary layer stagnation point and unique solution is obtained by the method of shooting algorithm. Thermal conductivity of the nanofluid across a vertically extending substrate with the uniform magnetic field influence with partial slip condition for the boundary layer flow problem's stagnation point had its wide application in the manufacturing industries for the cooling conditions with the effect of thermal and chemical reactions

---

*Corresponding author: E. Govindaraj

E-mail: *elatharasan@aucepkt.edu.in*

together with the slip conditions for the suction and injection [12, 13]. Enhancement of heat transfer with hybrid nanofluids for the magneto hydrodynamic flow of boundary layer with the implication of radiation and viscous dissipation in the porous medium to interpret velocity and temperature profile together with the augmentation of the non-Newtonian fluid was analysed. Experimental work for the impact of thermal radiation, heat generation, and cross-diffusion with Casson fluid in the porous material with the decrement in the magnetised field reduces the skin friction coefficient conditions over a curved surface [4 – 7].

There are many applications for this cutting-edge technological engineering development in the thermal and geothermal fields, oil reservoirs, and heat sinks in electronic chips. It examines issues with heat generation, thermal radiation, and viscous dissipation in boundary layers, demonstrating the properties and improvement of heat transport in porous media.

The enhanced thermal behaviour of nanofluids holds the promise of a significant leap in heat transfer intensification. Many studies on nanofluids are dedicated to delving deeper into their properties, with the aim of applying them in industrial settings where direct heat transfer improvement is crucial. Despite the considerable research on flow phenomena across a nonlinear stretching sheet, there is an urgent need for more work to fully comprehend the influence of pertinent parameters when using flow equations. The role of experimental design in the fields of research and engineering cannot be overstated. Its ability to determine the impact of independent variables on dependent variables is crucial, underscoring the significance of your work in the field.

Response surface methodology (RSM) is a leading experimental design for process optimization. This method not only demonstrates how input variables influence output variables, but also how they interact with each other, making it a practical and effective tool for your research.

Table 1. Characteristics of base and nanofluid [11, 18, 33, 34]

Property	Al_2O_3	Cu	H_2O
Density, $kg \cdot m^{-3}$	3970	8933	997.1
Thermal conductivity, $Wk^{-1}m^{-1}$	40	400	0.6071
Coefficient of thermal expansion, k^{-1}	.000051	.000076	.000256
Capacitance of heat, Jk^{-1}	765	385	4179

Comprehending the mechanisms of heat transmission facilitates the design of more effective systems, energy conservation, and the development of novel technologies. Heat transport is essential to many facets of our existence by developing sustainable solutions. Precise values of the physical and thermal parameters of the nanofluids, such as viscosity, specific heat, and thermal conductivity, are needed to investigate the heat transfer behaviour of the fluids are expressed in Table 2. Improved heat transfer results from the base fluid's thermo physical characteristics changing when these millimetre- or micrometre-sized particles are added. Nanofluids are being used in many different industries due to their special qualities, which include enhanced heat transfer performance and higher stability. According to researchers, the improved thermal

properties of the nanofluids, such as their increased thermal conductivity, specific heat, and viscosity among others are what have a favourable effect on thermal performance. The properties of nanofluid were experimentally validated from the published works [27, 31, 32].

Hybrid nanofluid provides a higher boost in thermo physical properties, especially in heat conductivity, as compared to the single or mono nanoparticle in the base fluid. Few studies have been conducted, and the literature only reports a few models for the characteristics of nano composite fluid. Table 3 showcases the correlation of the thermo-physical properties of the hybrid nanofluid.

Table 2. Thermo-physical attributes of nanofluid [27, 31, 32]

Property	Al_2O_3-H_2O/Cu-H_2O
Density of the fluid, kgm^{-3}	$\rho_{nf1} = \{(1 - \emptyset_{f1})\rho_{fl} + \emptyset_{1f}\rho_{s1}\}$ $\rho_{nf2} = \{(1 - \emptyset_{f2})\rho_{fl} + \emptyset_{2f}\rho_{s2}\}$
Heat capacitance, $k^{-1}J$	$(\rho cp)_{nf1} = \{(1 - \emptyset_{f1})(\rho cp)_{fl} + \emptyset_{1f}(\rho cp)_{s1}\}$ $(\rho cp)_{nf2} = \{(1 - \emptyset_{f2})(\rho cp)_{fl} + \emptyset_{2f}(\rho cp)_{s2}\}$
Thermal conductivity, $Wk^{-1}m^{-1}$	$\dfrac{k_{nf1}}{k_{fl}}$ $= \dfrac{\{k_{s1} + (n-1)k_{fl} - (n-1)\emptyset_{f1}(k_{fl} - k_{s1})\}}{\{k_{s1f} + (n-1)k_{fl} + \emptyset_{f1}(k_{fl} - k_{s1})\}}$ $\dfrac{k_{nf2}}{k_{fl}}$ $= \dfrac{\{k_{s2} + (n-1)k_{fl} - (n-1)\emptyset_{f2}(k_{fl} - k_{s2})\}}{\{k_{s2} + (n-1)k_{fl} + \emptyset_{f2}(k_{fl} - k_{s2})\}}$
Thermal expansion coefficient, k^{-1}	$\beta_{nf1} = \{(1 - \emptyset_{f1})(\beta)_{fl} + \emptyset_{f1}(\beta)_{s1}\}$ $\beta_{nf2} = \{(1 - \emptyset_{f2})(\beta)_{fl} + \emptyset_{f2}(\beta)_{s2}\}$

Table 3. Hybrid nanofluid [26, 32,33]– correlations

Property	Cu-Al_2O_3-H_2O
Density of fluid, $kg \cdot m^{-3}$	$\rho_{hnfl} = (1 - \emptyset_{f2})\{(1 - \emptyset_{f1})\rho_{fl} + \emptyset_{f1}\rho_{s1}\} + \emptyset_{f2}\rho_{s2}$
Heat capacitance, $k^{-1}J$	$(\rho c_p)_{hnfl} = (1 - \emptyset_{f2})\{(1 - \emptyset_{f1})(\rho c_p)_{fl} + \emptyset_{f1}(\rho cp)_{s1}\} + \emptyset_{f2}(\rho cp)_{s2}$
Thermal conductivity, $Wk^{-1}m^{-1}$	κ_{hnfl} $= \kappa_{nf}\left\{\dfrac{\kappa_{s2} + (n-1)\kappa_{fl} - (n-1)\emptyset_{f2}(\kappa_{fl} - \kappa_{s2})}{\kappa_{s2} + (n-1)\kappa_{fl} + \emptyset_2(\kappa_{fl} - \kappa_{s2})}\right\}$ κ_{nf} $= \kappa_{fl}\left\{\dfrac{\kappa_{s1} + (n-1)\kappa_{fl} - (n-1)\emptyset_{f1}(\kappa_{fl} - \kappa_{s1})}{\kappa_{s1} + (n-1)\kappa_{fl} + \emptyset_1(\kappa_{fl} - \kappa_{s1})}\right\}$
Thermal expansion coefficient, k^{-1}	$(\rho\beta)_{hnfl} = (1 - \emptyset_{f2})\{(1 - \emptyset_{f1})(\rho\beta)_{fl} + \emptyset_{f1}(\rho\beta)_{s1}\} + \emptyset_{f2}(\rho\beta)_{s2}$
Electrical conductivity, sm^{-1}	σ_{hnfl} $= \sigma_{nf}\left\{\dfrac{\sigma_{s2} + (n-1)\sigma_{fl} - (n-1)\emptyset_{f2}(\sigma_{fl} - \sigma_{s2})}{\sigma_{s2} + (n-1)\sigma_{fl} + \emptyset_2(\sigma_{fl} - \sigma_{s2})}\right\}$ σ_{nf} $= \sigma_{fl}\left\{\dfrac{\sigma_{s1} + (n-1)\sigma_{fl} - (n-1)\emptyset_{f1}(\sigma_{fl} - \sigma_{s1})}{\sigma_{s1} + (n-1)\sigma_{fl} + \emptyset_1(\sigma_{fl} - \sigma_{s1})}\right\}$
Dynamic viscosity, $kg \cdot m^{-1}s^{-1}$	$\mu_{hnfl} = \dfrac{\mu_{fl}}{(1 - \varphi_1)^{2.5}(1 - \varphi_2)^{2.5}}$

The objectives of the article are outlined as follows: heat transfer performance evaluation of the nanofluid over a surface of non-linearity with influential parameters is analysed.

8

1. The empirical model is designed to derive the optimisation of response factors.
2. The profile of temperature, quantity, and velocity histories are analysed to look for variations in the other quantities.
3. The response factors of velocity, temperature, Nusselt number and skin friction coefficient are validated with numerical algorithm for the range and contours are interpreted graphically and in tabular form.
4. The comparison of the existing results with the previous research work proved to have good agreements to the numerical and experimental schema.

2. MATHEMATICAL MODELLING – PROBLEM FORMULATION

The investigation examines incompressible two-dimensional flow over a stretched sheet with nonlinearity using a Cu-Al_2O_3-H_2O hybrid nanoparticle. It presents novel findings in fluid dynamics and nano-fluid mechanics. In Cartesian coordinates, the vertical axis y is perpendicular to the stretched surface, while the horizontal axis x is aligned with the surface's direction. The stretching parameter, denoted by n, characterizes the nanofluids' viscosity, and the velocity is defined as $a_1 x^n$, $a_1 > 0$. The Buongiorno model is employed to analyze the effects of Brownian motion14]. The equations for continuity, momentum, and energy are the governing equations, which are explained from Eq. 1 – Eq. 4, along with the initial and boundary conditions, and the parameters are resolved from Eq. 5 – Eq. 7.

The basic equations are defined as:

$$a_x + b_y = 0; \tag{1}$$

$$a\frac{\partial a}{\partial x} + b\frac{\partial a}{\partial y} = v_{nf}\frac{\partial^2 a}{\partial y^2} - \sigma\frac{B^2}{\rho_{nfl}}a.; \tag{2}$$

$$(\rho cp)_{nf}(a\frac{\partial T_1}{\partial x} + b\frac{\partial T_1}{\partial y} = k_{nf}\frac{\partial^2 T_1}{\partial y^2} + (\rho cp)_s[D_B\left(\frac{\partial}{\partial x}\frac{\partial \varphi}{\partial y} + \frac{D_T}{T_\infty}\left(\frac{\partial T_1}{\partial y}\right)^2\right] - \frac{\partial q_r}{\partial y} + \mu_{nf}(\frac{\partial a}{\partial y})^2; \tag{3}$$

$$a\frac{\partial \varphi}{\partial x} + b\frac{\partial \varphi}{\partial y} = D_B\frac{\partial^2 \varphi}{\partial y^2} - \frac{D_T}{T_\infty}\frac{\partial^2 T_1}{\partial y^2}. \tag{4}$$

The boundary conditions are considered as:

$$a=a = cx^n, b=0, \quad T_1 = T_w; \tag{5}$$

$$D_B\frac{\partial \varphi}{\partial y} + \frac{D_T}{T_\infty}\frac{\partial T_1}{\partial y} = 0; \tag{6}$$

Given y=0, a=0, $T_1 \to T_\infty, \varphi \to \varphi_\infty, as y \to \infty$. (7)

The variable magnetic field is defined as $B(x) = B_0 x^{\frac{(n-1)}{2}}$, where B_0 is a constant and independent of time with curl and the divergence of the vector is zero hence it is ir-rotational and solenoidal, and the vector is null. By Rooseland's approximations assuming the difference in the flow temperature T_4 as the Taylor's form and omitting the high powers [15]. The expansion of Taylor's is depicted in the Eq. 8 and Eq. 9.

We have

$$T_4 \approx 4T_\infty^3 T - 3T_\infty^4, q_r = \frac{-16\sigma^*}{3k^*}\left(T_1^3\frac{\partial T_1}{\partial y}\right). \tag{8}$$

Replacing T with T_l in the higher order expansion given by Taylor's approximations:

$$\frac{\partial q_r}{\partial x} = \frac{-16\sigma^*}{3k^*}\left(3T_1^2\left(\frac{\partial T_1}{\partial y}\right)^2 + T_1^3\frac{\partial^2 T_1}{\partial y^2}\right). \tag{9}$$

The dimensionless variable is characterized as

$$\Psi = \sqrt{\frac{2av_f}{n+1}}x^{\frac{(n+1)}{2}}f(\eta), \eta = y\sqrt{\frac{a(n+1)}{2v_f}}x^{\frac{(n-1)}{2}},$$

$$\theta(\eta) = \frac{T_1 - T_\infty}{T_w - T_\infty}, , \qquad \varphi(\eta) = \frac{\varphi - \varphi_\infty}{\varphi_\infty}. \tag{10}$$

Dimensionless stream function is outlined by

$$f(\eta), a = \frac{\partial \psi}{\partial y}, \quad b = -\frac{\partial \psi}{\partial x}. \tag{11}$$

The components of velocity are given by

$$a = a_1 x^n f'(\eta); \tag{12}$$

$$b = -\sqrt{\frac{a_1(n+1)v_f}{2}}x^{\frac{(n-1)}{2}}\left[f'(\eta)\eta\frac{n-1}{n+1} + f(\eta)\right]; \tag{13}$$

$$f''' + b_1\left[c_1\left(ff'' - \frac{2n}{n+1}f'^2\right) - M^2f'\right] = 0; \tag{14}$$

$$\theta''[1 + \frac{4k_f}{3N_R k_{nf}}(1 + (\theta_w - 1)\theta)^3 +$$
$$\frac{4k_f}{N_R k_{nf}}(1 + (\theta_w - 1)\theta)^2(\theta_w - 1)\theta'^2 -$$
$$\frac{k_f}{k_{nf}}[Pr c_2\left(f\theta' - \frac{4n}{n+1}f'\theta\right) + \frac{Pr Ec}{b_1}f''^2$$
$$+Nb\varphi'\theta' + Nt\theta'^2; \tag{15}$$

$$\varphi'' + Pr Lef\varphi' + \frac{Nt}{Nb}\theta'' = 0. \tag{16}$$

The equations in the similarity variables are solved for the velocity, volume concentration, and temperature are defined in Eq. 11 – Eq. 16. The values of the constant are given by Eq. 17. While the values are given by

$$b_1 = (1 - \varphi)^{-2.5}, c_1 = \left\{(1 - \varphi) + \varphi\left(\frac{\rho_s}{\rho_{fl}}\right)\right\}$$

$$c_2 = \{(1 - \varphi) + \varphi\left(\frac{(\rho cp)_s}{(\rho cp)_{fl}}\right)\}. \tag{17}$$

The boundary conditions are given by the Eq. 18 and Eq. 19.

$$f(0) = 0, \quad f'(0) = 1 = \theta(0)$$
$$Nb\varphi'(0) + Nt\theta'(0) = 0 \, at \eta = 0. \tag{18}$$

$$f'(\infty) = 0, \, as\theta(\infty) \& , \varphi(\infty) \to 0 \, with \eta \to \infty. \tag{19}$$

$$M^2 = \frac{2\sigma B_0^2}{a(n+1)\rho_f}; \tag{20}$$

$$Pr = \frac{v_f(\rho cp)_f}{k_f}, \quad Ec = \frac{U^2}{(cp)_f(T_w - T_\infty)}; \tag{21}$$

$$Nb = \frac{(\rho cp)_s D_B \varphi_\infty}{(\rho cp)_f \alpha_f}, Nt = \frac{(\rho cp)_s D_T(T_w - T_\infty)}{(\rho cp)_f \alpha_f T_\infty}$$

$$Le = \frac{\alpha_f}{D_B} N_R = \frac{16\sigma^* T_\infty^3}{3k^* k}. \tag{22}$$

The skin friction coefficient is defined as

$$c_f = \frac{\mu_{nf}\left(\frac{\partial u}{\partial y}\right)_{y=0}}{\rho_f U^2}; \tag{23}$$

$$c_f (Re_x)^{\frac{1}{2}} = \frac{\sqrt{n+1}}{(1-\varphi)^{2.5}} f''(0). \tag{24}$$

The values of M, Pr, Ec, Nb, N_t and the skin friction values are given by the Eq. 20 – Eq. 24 whereas the Nusselt values, Reynolds number, Heat transfer coefficient are given by Eq. 25 – Eq. 28 [16].

The Nusselt number is given by

$$Nu_x = \frac{q_w x}{k_f(T_w - T_\infty)}; \tag{25}$$

$$q_w = -\left(k_{nf} + \frac{16\sigma^* T^3}{3k^*}\right)\left(\frac{\partial T}{\partial y}\right)_{y=0}; \tag{26}$$

$$\frac{Nu_x}{\sqrt{Re_x}} = -\frac{k_{nf}}{k_f}\sqrt{n+1}\left[1 + \frac{k_f}{k_{nf}}\frac{4\theta_w^3}{3n_r}\right]\theta'(0); \tag{27}$$

$$Re_x = \frac{2ax^{n+1}}{v_f}. \tag{28}$$

The prime denotes differentiation to the similarity variable η.

3. RESULTS AND DISCUSSION

The magneto hydro dynamic boundary layer problem of nanofluid flow of 2D is analyzed for the mono [Cu, Al$_2$O$_3$] with base fluid and its hybrid [Cu-Al$_2$O$_3$-water] together with the boundary conditions taken for the nonlinear stretching surface under various parameters. The equations are solved for the solution numerically and are validated by the response surface methodology. The solutions obtained by considering the various parameters are interpreted graphically and compared with the results obtained earlier. The quantities are numerically interpreted for velocity and temperature distribution with varying values of magnetic measure in case of nonlinear stretching as expressed in Fig. 1 and Fig. 2. Table 4 displays the tabulated values that illustrate the profile of temperature, concentration, and velocity for various magnetic parameter values together with changes in the nonlinear stretching parameter at the initial values. The temperature and the velocity distribution profile are both enhanced with the increasing value of the nanoparticles' volume fraction, which directly raises boundary layer thickness and flow momentum, are explained in Fig. 3 and Fig. 4. When nanoparticles are added to the base fluid, it improves heat transmission. It increases the thermal conductivity of the nanofluid. The thickness related to the heat generation parameter resulting from the temperature increase has been projected in Fig. 5. Proportional increase in volume fraction successively enhances thermal conductance with small-molecule fluids [17].
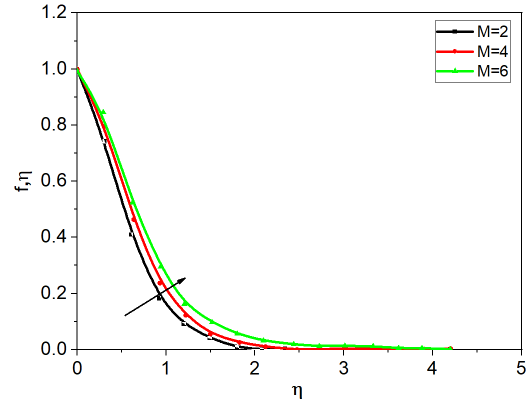
Fig. 1. Velocity profile with varying magnetic criterion
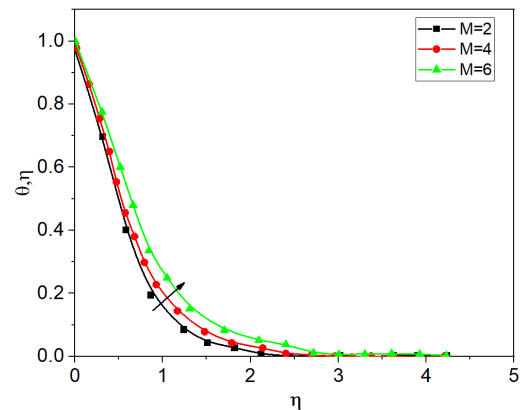
Fig. 2. Temperature distribution with magnetic parameter
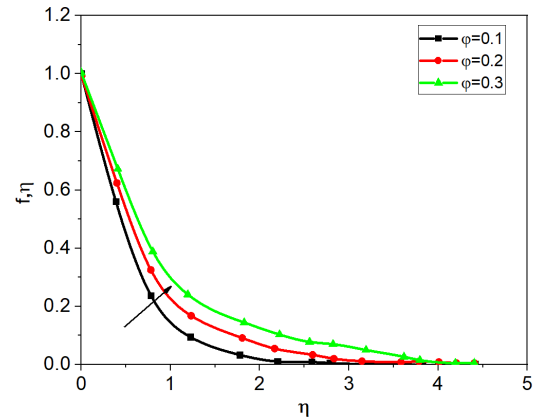
Fig. 3. Velocity distribution with concentration of nanoparticles

Table 4. Results of $f'(0), \theta'(0)$ for nanofluids [20, 28, 29]

n	M	Ø	$-\theta'(0)$				$-f''(0)$			
			Cu-H$_2$O	Al$_2$O$_3$-H$_2$O	Cu-Al$_2$O$_3$-H$_2$O Present/Previous	Error	Cu-H$_2$O	Al$_2$O$_3$-H$_2$O	Cu-Al$_2$O$_3$-H$_2$O Present/Previous	Error
1	1	0.1	0.017	0.015	0.010/0.009	-0.001	2.696	2.672	2.663/2.662	0.001
	2		0.008	0.005	0.004/0.0039	0.001	3.116	3.107	3.072/3.072	0.000
2	1		1.162	1.123	1.112/1.112	0.000	1.954	1.916	1.906/1.905	0.001
	2		0.856	0.814	0.764/0.7639	0.000	2.709	2.752	2.739/2.738	0.001
1	1	0.2	1.137	1.101	1.065/1.066	-0.001	3.545	3.504	3.499/3.500	-0.001
	2		0.722	0.725	0.706/0.706	0.000	4.232	4.211	4.194/4.193	0.001
2	1		1.019	1.006	1.088/1.087	0.001	3.011	2.897	2.843/2.842	0.001
	2		0.682	0.652	0.604/0.6039	0.001	2.459	2.416	2.395/2.394	0.001
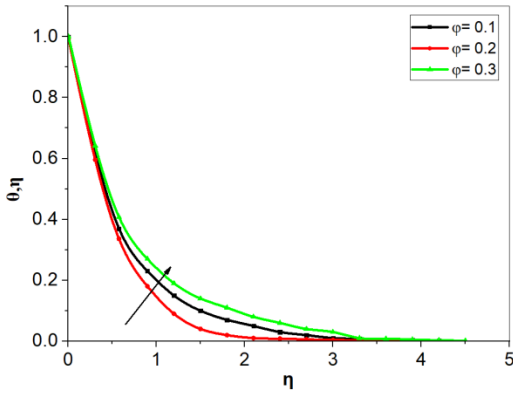
Fig. 4. Temperature profile with concentration of nanofluid
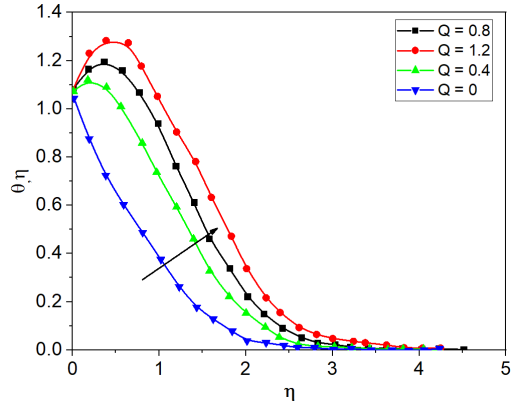
Fig. 5. Resultant of heat generation with temperature

The explanation provides insight into the nonlinear stretching parameter affects the velocity and temperature profile distributions in Fig. 6 and Fig. 7.
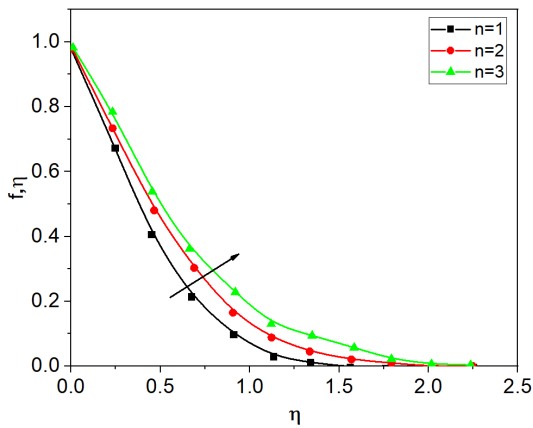
Fig. 6 Impact of nonlinear stretching criterion with velocity

Applying the Lorentz force improves the fluid flow. It shows that hybrid nanofluids are more efficient when the magnetic field element increases, the value of f'(η) falls, and the overall depth of the outermost boundary layer diminishes [18].

The literature provides validation for the current model. Das et al.'s [19] experimental research examined the critical function that temperature plays in enhancing nanofluid thermal conductivity. Hojjat et al. [21] conducted experiments to determine the significance of nanoparticle concentration and nanofluid temperature. In their investigation into the efficacy of nanofluid temperature,

Vajjha et al. [22] also claimed that a rise in temperature would improve the material's thermal attribute.
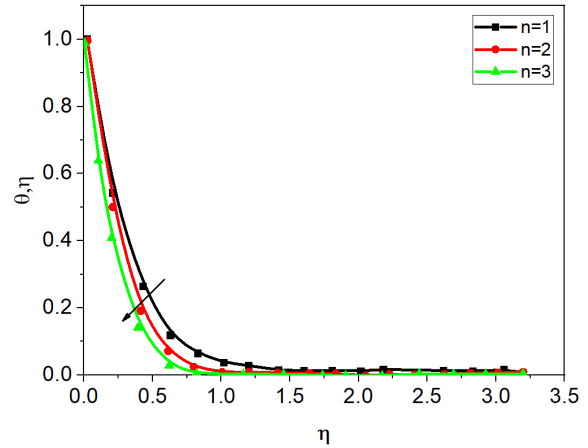
Fig. 7. Influence of nonlinear stretching criterion profile of temperature

Fig. 8 analyses the temperature profile with reference to the Prandtl number for different values of mono and hybrid nanofluid.
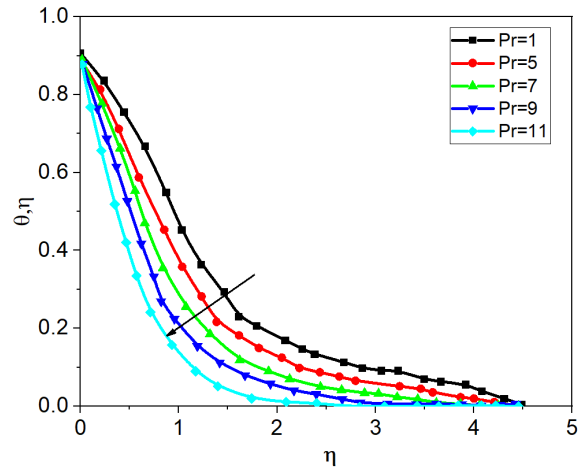
Fig. 8. Impact of Prandtl number with temperature profile

Significant parameters impact the momentum of the boundaries. Whereas the velocity profile and skin friction coefficient systematically rise alongside the temperature profile, the Nusselt number shows a considerable improvement correlating with a rise of the nano particle's volume fraction within the hybrid nanofluid [23]. Fig. 9 demonstrates the correlation between the predicted and the actual value, as the error can be minimised. The values of the skin friction coefficient are expressed graphically in Fig. 10 and tabulated in Table 5 for a range of magnetic parameter and nonlinear stretching parameter values. Utilising the Design Expert tool, the assessment of outcomes is done with the contours and surface plots for the input parameters nonlinear stretching, magnetic, concentration, Eckert number, and radiation. The impacts of process factors on the output response are experimented with analysis of variance. As per the findings of Battira et al. [24], temperature and volume fraction are the primary parameters that improve heat transmission.

According to Sajid et al. [25], hybrid nanofluids' thermal conductivity will rise with nanoparticle

concentration and temperature. The results are juxtaposed with existing literature. Aminreza et al. [26] indicated that the temperature and volume fraction are pivotal in increasing the thermal conductivity of nanofluids.
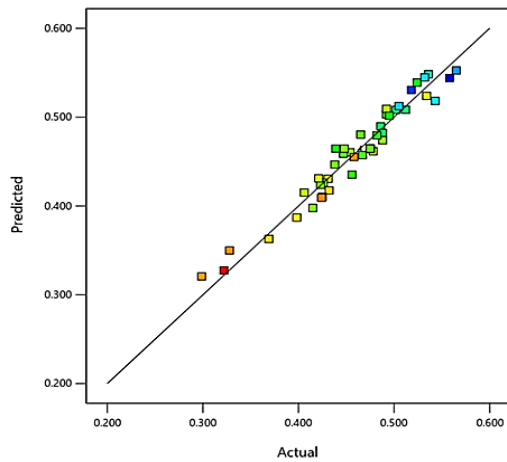
Fig. 9. Actual vs. predicted for temperature analysis

Palanisamy and Mukesh Kumar [27] experimentally found that a rise in volume fraction boosts the thermal conductivity of nanofluids. Notably, volume fraction percentages between 0.02 and 0.03 were observed to improve the thermal attribute of nanofluids; however, a further increase in volume fraction not yielded any additional improvements. These findings from the molecular dynamic studies on the thermal conductivity of nanofluids not only elucidate the factors affecting nanofluid thermal conductivity but also highlight a marked enhancement in heat transfer, which is one of the key findings of our research.

Table 5. Skin friction analysis

M	n	Nb	Nt	Cu-H_2O	Al_2O_3-H_2O	Cu-Al_2O_3-H_2O
0				11.12	11.24	11.28
1	10			8.85	9.72	9.93
2				6.21	7.10	7.21
	1	0.5		1.61	1.74	1.83
	2		0.5	2.75	3.2	3.4
	3			3.69	4.20	4.31
	10			7.47	8.32	8.41
1		0.1		7.48	8.40	8.50
		0.5		7.47	8.32	8.41
	10	0.7		7.46	8.28	8.24
		0.5	0.1	7.56	8.42	8.57
			0.5	7.47	8.32	8.41
			0.7	7.41	7.62	7.98

Both the mono and hybrid nanofluid's heat transmission rate is examined Cu-H_2O, Al_2O_3-H_2O and Cu-Al_2O_3-H_2O for the nonlinear stretching surface is expressed in Fig. 11 and Table 6. The operating design parameters are taken as nonlinear stretching parameter (A), magnetic parameter (B), concentration (C), Eckert number (D) and radiation parameter(E).

Table 6. Heat transfer rate analysis

M	n	Cu-H_2O	Al_2O_3-H_2O	Cu-Al_2O_3-H_2O
0	10	6.25	6.32	6.45
1		6.83	6.92	6.98
2		7.35	7.42	7.32
1	1	2.67	2.72	2.75
	2	3.52	3.61	3.72
	3	4.21	4.27	4.34
	10	6.83	6.92	6.98

Fig. 12 shows the normality of the residuals for the respective runs, which showcases the efficiency of the model with reference to skin friction's coefficient.

The hypothesis in the current work is formulated to demonstrate the improvement of heat transport in the non-linear stretching surface scenario for the magneto hydrodynamic nanofluid flow. The conclusions agree with the study conducted by Prasannakumara et al. [28] on the formulation of a two-phase slip of a dusty fluid flow containing nanoparticles over a non-linear stretching sheet implanted in the porous medium with the presence of non-linear thermal radiation. Hayat et al. [29] analysed a simulated model for the magneto hydro dynamic boundary flow of the fluid over a curvilinear surface of non-linearity. The properties of mass transmission and heat are experimented with using the features of chemical reactions and heat creation. Attributes of the various disparate specifications were examined for variations in temperature, concentration, skin friction coefficient, local Nusselt, Sherwood numbers, and velocity. The current work's numerical results do line up with the conclusions [29].

The study's goal is to significantly raise the temperature transmission while considering important factors by converting the governed partial differential equations combined with initial and boundary circumstances to the specific systemized transformation using ordinary differential equations of similarity and a quantitative scheme of computation acquired through the RK algorithm. The finite value of the similarity variable is selected to ensure that asymptotically, each boundary condition is met. Two distinct approximations of the solution are made at each step and contrasted. The approximation is approved if the two responses closely match. Else, the step size is decreased until the necessary preciseness [20].

Fig. 12 shows the normality of the residuals for the respective runs, which showcases the effectiveness of the prototype with reference to velocity. The F-value of the model 17.76 implies the model's relevance. Noise has a minimal 0.0001 % probability of producing a substantial F-value. Significant terms are indicated by P-values less than 0.0500. A, B, C, AB, AC, AE, and B² are important model terms in this case. Values above 0.1000 suggest that there is no significance for model terms. The substantial lack of fit is indicated by the 5.50-F-value. There is a good degree of agreement when the Adjusted R^2 of 0.8816 and the Predicted R2 of 0.7443 deviate by less than 0.2.
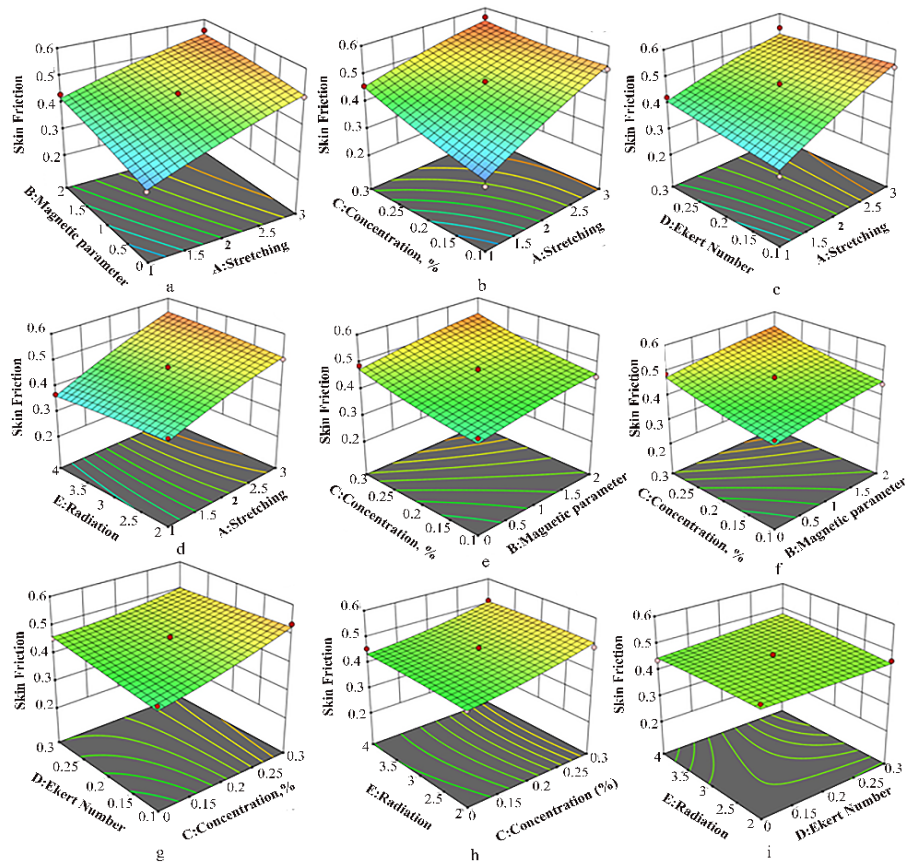
Fig. 10. Skin friction 3D Interaction analysis for response factors a-AB, b-AC, c-AD, d-AE, e-BC, f-BC, g-CD, h-CE, i-DE
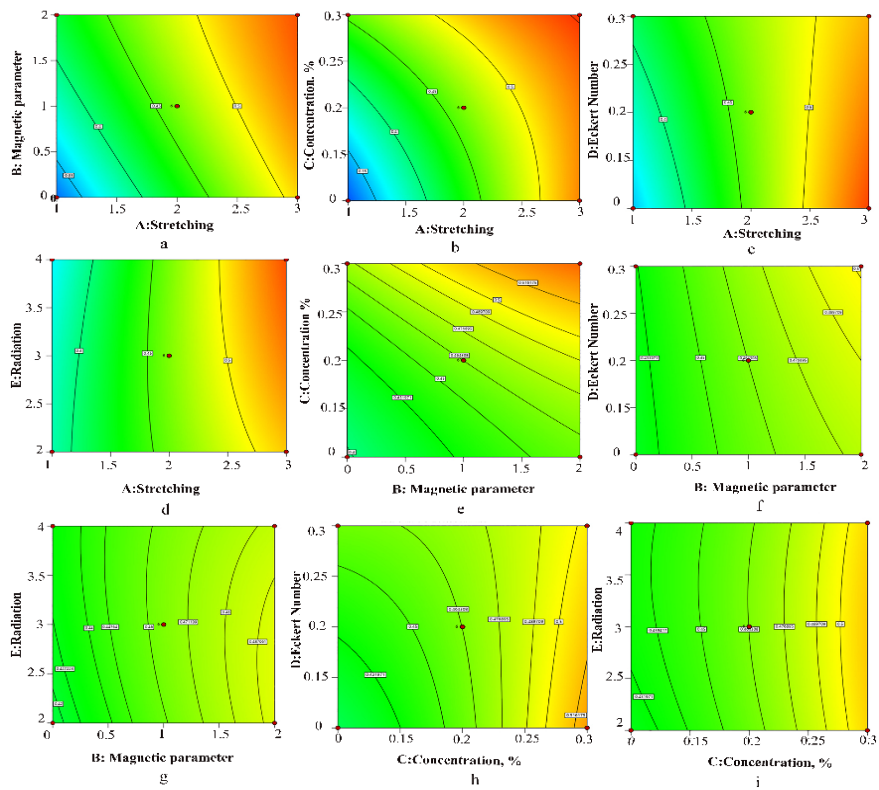
Fig. 11. Heat transfer coefficient analysis for response factors a-AB, b-AC, c-AD, d-AE, e-BC, f-BD, g-BE, h-CD, i-CE
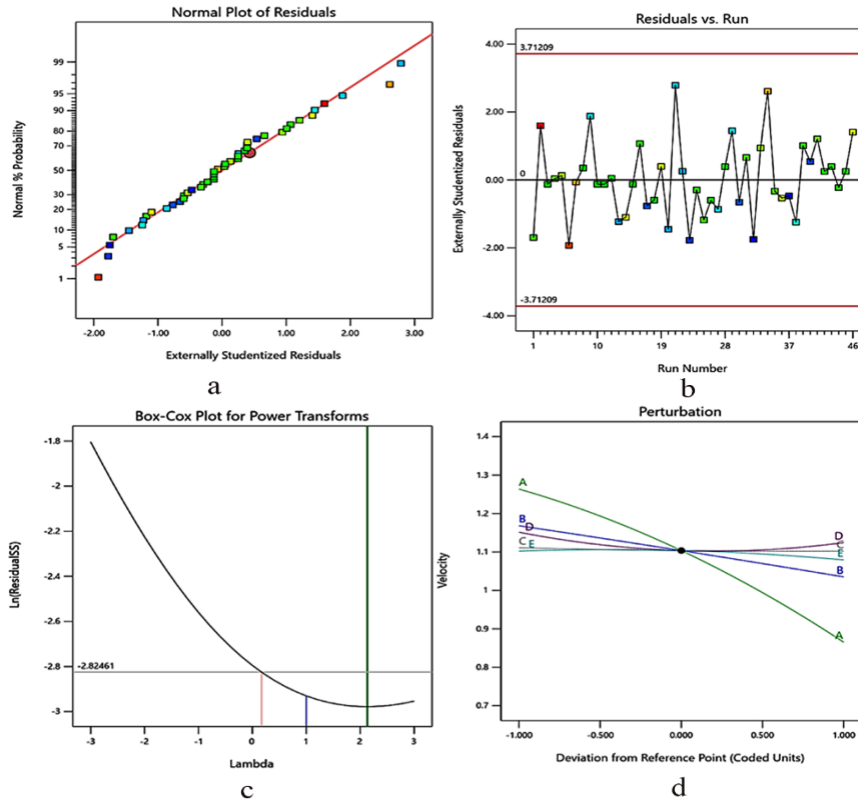
Fig.12. Diagnostic plots of velocity contours for: a – residuals; b – runs; c – box-cox; d – perturbation

Table 7. Temperature distribution with impact of influential parameters– Analysis of variance (ANOVA)

Origin	Sum of squares	DF	Mean sumof squares	Ratio-F	P-value
Model	0.0956	20	0.0048	21.69	< 0.0001
Factor A	0.0728		0.0728	330.11	< 0.0001
Factor B	0.0086		0.0086	39.24	< 0.0001
Factor C	0.0028		0.0028	12.74	0.0015
Factor D	0.0004		0.0004	1.86	0.1847
Factor E	0.0001		0.0001	0.5002	0.4860
Factors AB	0.0005		0.0005	2.10	0.1600
Factors AC	0.0002		0.0002	1.09	0.3065
Factors AD	0.0002		0.0002	0.7667	0.3896
Factors AE	0.0004		0.0004	1.91	0.1796
Factors BC	0.0000	1	0.0000	0.0556	0.8156
Factors BD	0.0000		0.0000	0.1633	0.6896
Factors BE	9.000E-06		9.000E-06	0.0408	0.8415
Factors CD	0.0001		0.0001	0.2552	0.6179
Factors CE	0.0008		0.0008	3.43	0.0758
Factors DE	0.0001		0.0001	0.2903	0.5948
FactorsA²	0.0067		0.0067	30.21	< 0.0001
FactorsB²	0.0003		0.0003	1.29	0.2668
FactorsC²	3.409E-06		3.409E-06	0.0155	0.9020
FactorsD²	0.0001		0.0001	0.4966	0.4875
FactorsE²	0.0000		0.0000	0.2079	0.6523
Residual	0.0055	25	0.0002		
Lack of fit	0.0055	20	3×10^{-3}	43.49	
Pure error	0.0000	5	6.300E-06		
Cor total	0.1011	45			

The 17.0312 ratio suggests a strong enough signal, inspiring the exploration of the design space using this fitted model. The Cu-water nano-fluid in a jet impingement on heated transferring plates was analysed using a computational model of heat transmission. Experiment analysis of the distribution of velocity, and concentration considering the fluctuation of the Reynolds number with distance from the jet's nozzle to the plate was performed. The correlation analysis of the Nusselt number and coefficient of skin friction was tabulated to explain the heat transmission and movement of fluids. A qualitative examination of stream functional mechanisms and thermal-isotherm contours is studied to comprehend heat transfer mechanism and flow pattern resulting from the surface by Datta et al. [30].

The F-value 21.69 indicates the model's importance. The likelihood that noise will result in a significant F-value is approximately 0.01 %. For model terms, P-values less than 0.0500 indicate significance. The design's standard deviation is 0.0148, with a mean of 0.8728 and a coefficient of variation of 1.7.

The R² value is calculated as 94.55 %, with the adjusted and predicted values at 90.19 % and 78.28 % respectively. The model's precision, indicated by 18.3923, is the best fit for the temperature analysis, as shown in Table 7, instilling confidence in its reliability.

4. CONCLUSIONS

The study analyses the MHD properties of the nanofluid over a stretched sheet that is not linear, and the governing parameters of the flow are examined. The governing PDEs are changed to ODEs by transformation of similarity. The results are showcased using an analytical method and compared with the established literature for the response factors taken for the present study, and higher precision of accuracy is established.

The investigation has been conducted analytically to demonstrate the enhancement of heat transmission in nanofluids across a nonlinear stretching surface with operating parameters. The thermal efficiency has been analyzed using numerical and statistical evaluation to determine the effect of design and operating parameters on its optimum.

The model's fit is analyzed using the response surface methodology with analysis of variance in design expert software. The quantitative findings indicate that improving the governing factors generates advancements in flow and warmth.

The pertinent parameters exhibited in tabular and graphical form influence the statistical inference of the response factors (heat transfer rate, skin friction coefficient, and temperature contour and velocity distribution).

The findings obtained from the study are summed up as follows:

1. Regarding the coefficient of skin friction, a rise in the parameters for nonlinear stretching and magnetic fields acts in the exact opposite way: diminishing the velocity distribution. Temperature distributions are inversely correlated with increases in the nonlinear stretching and magnetic criterion, respectively.

2. The decreased skin friction coefficient of nanofluid volume fraction shoots up as the magnetic parameter escalates.

3. The temperature distribution grows with a rise in the radiation and heat-generating parameters.

4. The upsurge in radiation parameter enhances skin friction, and the pace of heat transference diminishes with an increment in the non-stretching parameter, the volume of the nanofluid, and the Prandtl number.

5. Heat transfer reduces with an upsurge in the magnetic measure and the layer's thickness at the boundary of momentum, diminishing with an increasing thickness of the thermal depth layer and fluid concentration.

6. As the warmth of the boundary with the nanofluid rises, the velocity profile falls, and skin friction rises. It is established that the upsurge in the proportion of the nanofluid's volume improves the temperature profile and velocity.

7. The elevation of the Brownian motion parameter examines the relationship between the layer's thickness at the boundaries and the rate of heat transfer. The Brownian parameter lessens the effect on temperature distribution.

8. A high coefficient of determination indicates that the model accurately captures variations in the heat transmission rate through chosen parameters.

9. The percentage of the nanofluid's volume escalates with the increasing thermophoresis and a magnetic interaction parameter.

10. The fittest model of the skin friction coefficient is significant because it is overall optimal. The factors of nonlinear stretching, concentration, and a magnetic parameter, together with their interactions, have a significant P-value below 0.05, which is evident that the model is optimized.

11. The present model for the rate of heat transference is significant as it has overall optimization, specifically with the interactions of magnetic, concentration,

radiation, and nonlinear stretching factors. The model's F value of 24.34 % proves its efficiency.

12. The standard deviation for the response factors is given by 0.0174(heat transfer rate) and 0.0173(skin friction's coefficient) demonstrates convergence of the solution.

Nomenclature

Name	Significance	Unit
x	Dimensionless Cartesian coordinate parallel to the sheet	
y	Dimensionless coordinate perpendicular to the sheet	
a, b	Velocity x, y components	ms^{-1}
Re	Reynolds number	
T	Temperature of the fluid	K
Pr	Prandtl number	
Ec	Eckert number	
B_0	Strength of magnetic field	$kg.s^{-2}m^{-1}$
q_r	Radiative heat flux	Wm^{-2}
M	Magnetic number	
C_p	Specific heat constant pressure	$Jkgk^{-1}$
Nu	Nusselt number	
C_f	Skin friction coefficient	
η	Similarity variable	
Nb	Brownian parameter	
Nt	Thermophoresis parameter	
Le	Lewis number	
D_B	Brownian diffusion coefficient	m^2s^{-1}
D_T	Thermophoresis coefficient	m^2s^{-1}
$f(\eta)$	Dimensionless stream velocity	
$\theta(\eta)$	Dimensionless temperature profile	
$\phi(\eta)$	Dimensionless concentration profile	
φ	Nanoparticles volume fraction	
ρ	Density of the fluid	kgm^{-3}
ϑ	Kinematic viscosity	m^2s^{-1}
σ	Electric conductivity	sm^{-1}
α	Thermal diffusivity	m^2s^{-1}
β	Volumetric thermal expansion coefficient	k^{-1}
κ	Thermal conductivity	$Wm^{-1}k^{-1}$
μ	Dynamic viscosity	$kgm^{-1}s^{-1}$
σ^*	Stefan-Boltzmann constant	$m^2kgs^{-2}k^{-1}$
k^*	Rooseland coefficient of mean absorption	
τ	Ratio of effective heat capacity of fluid and nanoparticles	
ψ	Stream function	
N_R	Thermal radiation	
fl	Base fluid	
nf	Nanofluid	
$hnfl$	Hybrid nanofluid	
$f1, f2$	Fluids of Alumina and Copper	
s	Solid particles	
$s1$	Aluminium oxide nanoparticles	
$s2$	Copper nanoparticles	
w	Sheet surface conditions	
∞	Free stream condition	
RK	Runge-Kutta	
RSM	Response Surface Methodology	
PDE	Partial Differential Equations	
ODE	Ordinary Differential Equations	
MHD	Magneto Hydrodynamic	
ANOVA	Analysis of Variance	
DF	Degrees of freedom	

REFERENCES

1. **Choi, S.U.S., Zhang, Z.G., Yu, W., Lockwood, F.E., Grulke, E.A.** Anomalous Thermal Conductivity Enhancement in Nanotubes Suspensions *Applied Physics Letters* 79 2001: pp. 2252 – 2254.
https://doi.org/10.1063/1.1408272

2. **Xuan, Y., Li, Q.** Investigation on Convective Heat Transfer and Flow Features of Nanofluids *Journal of Heat Transfer, Transactions of the ASME* 125 2003: pp. 151 – 155.
https://doi.org/10.1115/1.1532008

3. **Rana, P., Bhargava, R.** Flow and Heat Transfer of a Nanofluid over a Nonlinearly Stretching Sheet: A Numerical Study *Communications in Nonlinear Science and Numerical Simulation* 17 2012: pp. 212 – 226.
https://doi.org/10.1016/j.cnsns.2011.05.009

4. **Ramesh, G.K., Prasannakumara, B.C., Gireeshaand, B.J., Rashidi, M.M.** Casson Fluid Flow near the Stagnation Point over a Stretching Sheet with Variable Thickness and Radiation *Journal of Applied Fluid Mechanics* 9 (3) 2016: pp. 1115 – 1122.
https://doi.org/10.18869/acadpub.jafm.68.228.24584

5. **Turkyilmazoglu, M.** Magneto Hydrodynamic Two-Phase Dusty Fluid Flow and Heat Model over Deforming Isothermal Surfaces *Physics of Fluids* 29 2017: pp. 013302.
https://doi.org/10.1063/1.4965926

6. **Abbas, Z., Naveed, M., Sajid, M.** Hydromagnetic slip flow of Nanofluid over a Curved Stretching Surface with Heat Generation and Thermal Radiation *Journal of Molecular Liquids* 215 2016: pp. 756 – 762.
https://doi.org/10.1016/j.molliq.2016.01.012

7. **Khan, M., Malik, R., Munir, A., Khan, W.A.** Flow and Heat Transfer to Sisko Nanofluid Over a Nonlinear Stretching Sheet *PLoS ONE* 10 (5) 2015: pp. e0125683.
https://doi.org/10.1371/journal.pone.0125683

8. **Ramya, D., Srinivasa Raju, R., Anand Rao, J.** Influence of Chemical Reaction on MHD Boundary Layer Flow of Nanofluids over a Nonlinear Stretching Sheet with Thermal Radiation *Journal of Nanofluids* 5 (6) 2016: pp. 880 – 888.
https://doi.org/10.1166/jon.2016.1276

9. **Hayat, T., Aziz, A., Muhammad, T., Alsaedi, A.** On Magneto Hydrodynamic Three-Dimensional Flow of Nanofluid Over a Convectively Heated Nonlinear Stretching Surface *International Journal of Heat and Mass Transfer* 100 2016: pp. 566 – 572.
https://doi.org/10.1016/j.ijheatmasstransfer.2016.04.113

10. **Bhuvaneswari, S., Elatharasan, G.** Numerical Methods of Solving One Dimensional Heat Equation Comparative Study *Journal of Applied Science and Computations* 6 2019: pp. 976 – 982.
https://doi.org/16.10089.jasc.2018.V613.453459.150010378

11. **Bhuvaneswari, S., Elatharasan, G.** An Experimental Investigation of Heat Transfer in Heat Exchangers Using Al_2O_3 Nanofluid © Springer Nature Singapore Pte Ltd. 2021 E. T. Akinlabi et al. (eds.) *Trends in Mechanical and Biomedical Design* Lecture Notes in Mechanical Engineering 2021: pp. 775 – 783.
https://doi.org/10.1007/978-981-15-4488-0_65

12. **Bhuvaneswari, S., Elatharasan, G.** Numerical Study of Heat Transfer and Pressure Drop in a Helically Coiled Tubes© Springer Nature Singapore Pte Ltd. 2021 E. T. Akinlabi et al. (eds.), *Trends in Mechanical and Biomedical Design* Lecture Notes in Mechanical Engineering 2021: pp. 785 – 796.
https://doi.org/10.1007/978-981-15-4488-0_66

13. **Haroun, N.A.H., Mondal, S., Sibanda, P.** Hydro magnetic Nanofluids flow through a Porous medium with Thermal Radiation, Chemical Reaction and Viscous Dissipation using the Spectral Relaxation Method International *Journal of Computational Methods* 16 (6) 2019: pp. 1840020
https://doi.org/10.1142/S0219876218400200

14. **Khan, S.U., Shehzad, S.A.** Brownian Movement and Thermophoretic Aspects in Third-grade Nanofluid Over Oscillatory Moving Sheet *Physica Scripta* 94 (9) 2019: pp. 095202.
https://doi.org/10.1088/1402-4896/ab0661

15. **Patel, H.R.** Effects of Cross Diffusion and Heat Generation on Mixed Convective MHD flow of Casson fluid through Porous Medium with Non-linear Thermal Radiation *Heliyon* 5 (4) 2019: pp. e01555.
https://doi.org/10.1016/j.heliyon.2019.e01555

16. **Geng, Y., Hassan, A., Monfared, M., Moradi, R.** MHD Nanofluid Heat Transfer between a Stretching Sheet and a Porous Surface Using Neural Network Approach *International Journal of Modern Physics C* 30 2019: pp. 1950048.
https://doi.org/10.1142/S0129183119500487

17. **Jamaludin, A., Nazar, R., Pop, I.**.Three-Dimensional Magneto Hydrodynamic Mixed Convection Flow of Nanofluids Over a Nonlinearly Permeable Stretching/Shrinking Sheet with Velocity and Thermal Slip *Applied Sciences* 8 2018: pp. 1128.
https://doi.org/10.3390/app8071128

18. **Mukesh Kumar, P.C., Arun Kumar, C.M.** Numerical Study on Heat Transfer Performance usingAl_2O_3/water Nanofluids in Six Circular Channel Heat Sink for Electronic Chip *Materials Today: Proceedings* 21 2020: pp. 194 – 201.
https://doi.org/10.1016/j.matpr.2019.0.220

19. **Das, S.K., Putra, N., Thiesen, P., Roetzel, W.** Temperature Dependence of Thermal Conductivity Enhancement for Nanofluids *Journal of Heat Transfer* 2003: pp. 567 – 574.
https://doi.org/10.1115/1.1571080

20. **Mansur, S., Anuar I., Pop, I.** Stagnation-Point flow towards a Stretching/Shrinking sheet in a Nanofluid using Buongiorno's Model *Proceedings of the Institution of Mechanical Engineers Part E Journal of Process Mechanical Engineering* 231 2017: pp. 172 – 180.
https://doi.org/10.1177/0954408915585047

21. **Hojjat, M., Etemad, S.Gh., Bagheri, R., Thibault, J.** Thermal Conductivity of Non Newtonian Nanofluids: Experimental Data and Modeling using Neural Network *International Journal of Heat and Mass Transfer* 54 2011: pp. 1017 – 1023.
https://doi.org/10.1016/j.ijheatmasstransfer.2010.11.039

22. **Vajjha, R.S., Das, D.K.** Experimental determination of Thermal conductivity of Three Nanofluids and Development of New Correlations *International Journal of Heat and Mass Transfer* 52 (21 – 22) 2009: pp. 4675 – 4682.
https://doi.org/10./j.ijheatmasstransfer.2009.06.027

23. **Tajik Jamal-Abadi, M., Zamzamian, A.H.** Optimization of Thermal Conductivity of Al_2O_3 Nanofluid by using ANN and GRG Methods *International Journal of Nanoscience and Nanotechnology* 9 (4) 2013: pp. 177 – 184.

24. **Battira, M., Bessaïh, R.** Radial and Axial Magnetic fields effects on Natural Convection in a Nanofluid-filled Vertical Cylinder *Journal of Applied Fluid Mechanics* 9 (1) 2016: pp. 407 – 418.
https://doi.org/10.18869/acadpub.jafm.68.224.24187

25. **Sajid, M., Ali, H.** Thermal Conductivity of Hybrid Nanofluids: A Critical Review *International Journal of Heat and Mass Transfe*r 126 2018: pp. 211 – 234.
https://doi.org/10.1016/j.ijheatmasstransfer.2018.05.021

26. **Noghrehabadi, A., Pourrajab, R.** Experimental Investigation of Forced Convective Heat Transfer Enhancement of γ-Al_2O_3/water Nanofluid in a Tube *Journal of Mechanical Science and Technology* 30 (2) 2016: pp. 943 – 952.
http://dx.doi.org/10.1007/s12206-016-0148-z

27. **Palanisamy, K., Mukesh Kumar, P.C.** Heat Transfer Enhancement and Pressure Drop Analysis of a Cone Helical Coiled Tube Heat Exchanger using MWCNT/Water Nanofluid *Journal of Applied Fluid Mechanics* 10 2017: pp. 7 – 13.
https://doi.org/10.36884/jafm.10.SI.28265

28. **Prasannakumara, B.C., Shashikumar, N.S., Venkatesh, P.** Boundary Layer Flow and Heat Transfer of Fluid Particle Suspension with Nanoparticles Over a Nonlinear Sheet Embedded in a Porous Medium *Nonlinear Engineering* 6 (3) 2017: pp. 179 – 190.
https://doi.org/10.1515/nleng-2017-0004

29. **Hayat, T., Saif, R., Ellahi, R., Muhammad, T., Ahmad, B.** Numerical Study of Boundary-Layer flow due to a Nonlinear Curved Stretching Sheet with Convective Heat and Mass Conditions *Results in Physics* 7 2017: pp. 2601 – 2606.
http://dx.doi.org/10.1016/j.rinp.2017.07.023

30. **Datta, A., Kumar, S., Halder, P.** Heat Transfer and Thermal Characteristics Effects on Moving Plate Impinging from Cu-Water Nanofluid Jet *Journal of Thermal Science* 29 2020: pp. 182 – 193.
https://doi.org/10.1007/s11630-019-1107-7

31. **Ezhil, K., Thavada, S., Ramakrishna, S.** MHD Slip Flow and Heat Transfer of Cu-Fe_3O_4 Ethylene Glycol-Based Hybrid Nanofluid over a Stretching Surface *Bio Interface Research in Applied Chemistry* 11 (4) 2021: pp. 11956 – 11968.
https://doi.org/10.33263/briac114.1195611968

32. **Suriya Uma Devi, S., Anjali Devi, S.P.** Numerical Investigation of Three Dimensional Hybrid Cu-Al_2O_3/water Nanofluid Flow Over a Stretching Sheet with Effecting Lorentz Force Subject to Newtonian Heating *Canadian Journal of Physics* 94 (5) 2016: pp. 490 – 496.
https://doi.org/10.1139/cjp-2015-0799

33. **Hayat, T., Nadeem, S.** Heat Transfer Enhancement with Ag-CuO/water Hybrid Nanofluid *Results in Physics* 7 2017: pp. 2317 – 2324.
https://doi.org/10.1016/j.rinp.2017.06.034

34. **Sheikholeslami, M., Hatami, M., Ganji, D.D.** Nanofluid Flow and Heat Transfer in a Rotating system in the presence of a Magnetic Field *Journal of Molecular Liquids* 190 2014: pp. 112 – 120.
https://doi.org/10.1016/j.molliq.2013.11.002

35. **Mabood, F., Khan, W.A., Ismail, A.I.M.** MHD Boundary Layer Flow and Heat Transfer of Nanofluids over a Nonlinear Stretching Sheet: A Numerical Study *Journal of Magnetism and Magnetic Materials* 374 2015: pp. 569 – 576.
https://doi.org/10.1016/j.jmmm.2014.09.013